Invited Paper

SIZE EFFECT OF THE CONCRETE CONE FAILURE LOAD OF ANCHOR BOLTS

ROLF ELIGEHAUSEN
Professor/Institut für Werkstoffe im Bauwesen,
Stuttgart University, Germany

PETR BOUŠKA
Research Engineer/Klokner Institute
Czech Technical University of Prague, CSFR

VLADIMIR ČERVENKA
Červenka Consulting, Prague, CSFR

RADOMÍR PUKL
Research Engineer/Klokner Institute

ABSTRACT

The concrete cone capacity of headed anchor bolts subjected to axial tension load was experimentally investigated using 35 concrete specimens of three different sizes. The dimensions of the test specimens were varied in proportion to the embedment depth h (h = 50, 150 and 450 mm). Material properties were measured on accompanying specimens. The measured failure loads are compared with other experimental and numerical investigations. According to the present results the failure loads increase in proportion to $h^{1.6}$, that means close to the prediction by linear fracture mechanics.

INTRODUCTION

Fastening elements such as headed-, expansion- and undercut anchors are often used in the construction industry to transfer loads into concrete structures. The design of such fastenings is mainly based on the results of experimental investigations [3]. One of the open problems is the so-called size effect of the concrete cone failure load.

An experimental investigation of the pull-out strength of headed anchors was recently conducted at the Klokner Institute of the Czech Technical University in Prague in cooperation with the Institute for Building Materials of the Stuttgart University. The main objective of the investigation was to verify the size effect of the concrete cone failure load.

EXPERIMENTAL PROGRAM

Specimens and headed anchor bolts of three different sizes of the same geometrical shape were used. For corresponding dimensions the ratio 1 : 3 : 9 was applied, while the actual embedment length was 50, 150 and 450 mm. Furthermore two different diameters of the anchor heads were used. All specimens were made from concrete of nominally identical quality with a specified cube strength $f_{cc} = 30$ MPa. The specimens were cast in six series. Each series of specimens was cast from the same concrete mix, 18 specimens were tested in series I to III [1] and 17 specimens in series IV to VI [2].

TEST SPECIMENS

The shape of the specimens in plan view was a square (small and medium sizes of series I to III) or an octagon respectively (all other specimens). The dimensions of the specimens are shown in Fig. 1 and listed in Table 1. The diameter of head type A was with $d_h \sim 1.9\, d_0$ (d_0 = shaft diameter) relatively large. For head type B the head diameter d_h was chosen such that the stresses under the head at peak load were kept almost constant ($\sigma_u \sim 14\, f_{cc}$). The concrete mix was transported from an industrial plant by mobil mixers to the laboratory, where the specimens were cast. Composition and properties of the mix are described in Table 2. The results of the accompanying material tests (average value of at least 3 tests) performed at the time of testing (concrete age about 45 days), are also given in Table 2. To avoid a splitting failure the specimens of series I to III were reinforced by an orthogonal ribbed reinforcement placed near the top surface and anchored by hooks. In series IV to VI the specimens were constrained by a welded orthogonal steel frame which was placed around the top of the specimens and slightly prestressed to ensure direct contact.

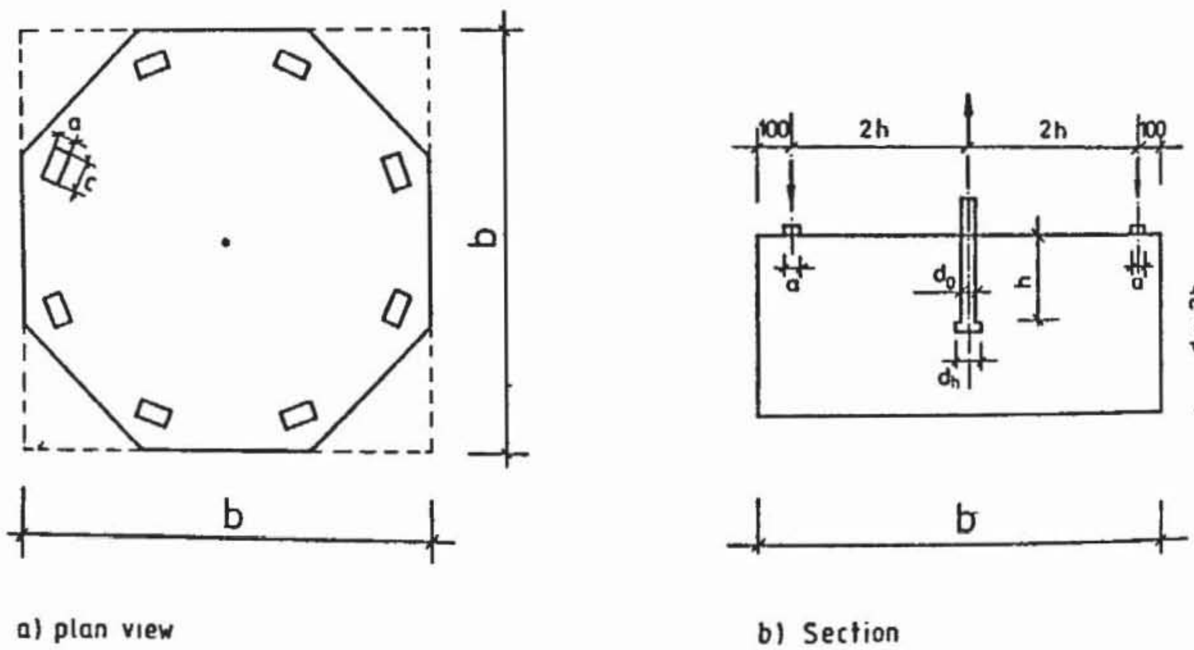

Fig. 1 Test specimen

TEST PROCEDURE

The tensile force was transferred to the anchor through a shaft with two spherical hinges to minimize bending moments on the anchor. Three types of loading systems were used: for small specimens 100 kN hydraulic machine Amsler, for medium specimens a pair of 250 kN jacks and for large specimens a pair of 1500 kN jacks. However, in series I to III the anchor bolts with h = 50 mm ruptured before a concrete cone was formed because of a too low steel strength. Therefore a hole was drilled from the back side of the specimens and the anchors were loaded by a compression force on the anchor head. In all other tests the anchor bolts did not yield. The support reaction was taken up by a special orthogonal structure resting on eight supports located on a circle (see Fig. 1).

TABLE 1
Dimension of specimens in mm

Size	Anchor				Specimen		Support	
			d_h					
	h	d_0	head A	head B	b	d	a	c
small	50	8	15.0	12.7	400	100	10	40
medium	150	24	45.6	32.9	800	300	30	100
large	450	72	135.5	88.5	2000	900	100	180

TABLE 2
Concrete mix and properties

Series	Cement[1]	Water	W/C	Aggregates[2] size in mm		Ligo-plast SF	Slump	f_{cc} [3]	f_t [4]	E_c	G_f [5]
				0 - 4	8 - 22						
	kg/m³	kg/m³		kg/m³	kg/m³	kg/m³	mm	MPa	MPa	GPa	N/m
I	350	195	0.57	890	905	2	110	32.6	2.97	26.2	169
II								29.7	2.85	29.8	170
III								33.2	3.00	26.4	167
IV	350	200	0.58	880	890	2	150	29.3	2.76	30.1	126
V								28.3	3.09	30.5	146
VI								34.4	3.17	31.5	152

1) Slag-Portland cement SPC 325
2) natural round aggregates
3) measured on cubes (side length 200 mm)
4) tensile splitting strength
5) measured on notched beams (d = 100 mm) in 3 point bending according to RILEM [11]

The loading was performed under displacement control by manual operation of the hydraulic system. The time-displacement relation was kept approximately linear. For each size of specimen a special calibrated load cell was used. During the test the anchor load, the relative displacement between the loaded end of the anchor bolt and the top surface of the specimen and the strains on the surface of the shaft were measured by Peekel Instruments data acquisition system Autolog controlled by a PDP computer 11/23. In series IV to VI also the displacement of the anchor head was measured.

TEST RESULTS

In all tests failure was caused by pushing (Series I to III, h = 50 mm) or pulling out (all other tests) a concrete cone. The shape of this cone was approximately similar for all embedment depths. In general the diameter of the cone on the concrete surface was < 4h. However, in some tests with large anchors (h = 450 mm), the formation of the failure cone was restricted by the supports.

In Fig. 2 typical load displacement curves for anchors with head type B and an embedment depth h = 50, 150 and 450 mm are plotted. In Table 3 the concrete cone failure load of anchors with head type B are listed. The concrete compression strength varied between 28 and 34 MPa. Therefore the failure loads were normalized to the average compression strength f_{cc} = 31 MPa by multiplying the measured values with the factor $(31/f_{cc})^{0.5}$. The weighted coefficient of variation of the normalized failure loads amounts to V ~ 11 %. This coefficient of variation is quite common for such tests. A much larger value must be expected, if the concrete mix is varied. For anchors with a larger head (type A), the average failure load was 10 % (h = 50 mm), 14 % (h = 150 mm) and 6 % (h = 450 mm) higher than for anchors with head type B. This is due to the much smaller concrete stresses under the head at peak load (~ 3.6 (h = 450 mm) to 8.6 f_{cc} (h = 50 mm)) which lead to smaller displacements of the anchors with a larger head.

The test results for the deepest anchors (h = 450 mm) might have been influenced favourably by two effects: (1) The concrete compression strength was measured on cubes which were cured as the test specimens. Because of hydration heat generated in the large specimens, the concrete strength might have been somewhat higher than measured on control specimens. (2) In some tests, the formation of the failure cone was hindered by the supports. However, it is believed that the combined effect of both influencing factors is small.

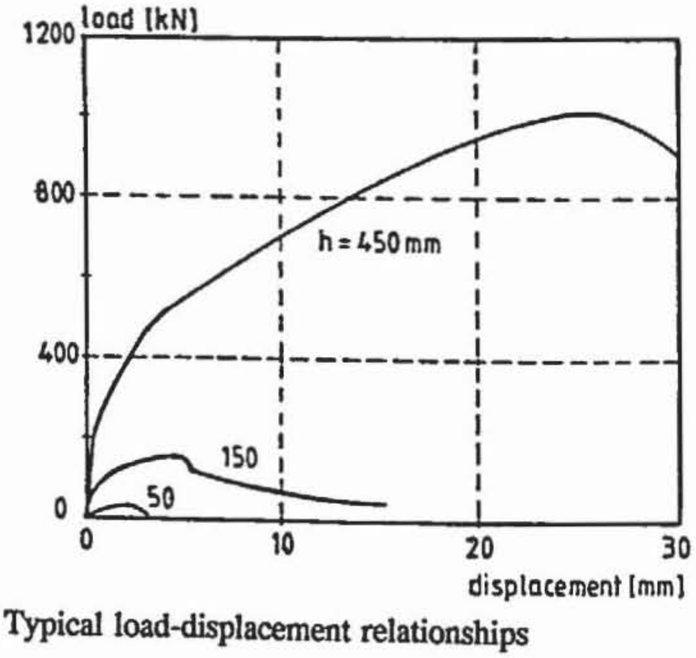

Fig. 2 Typical load-displacement relationships

TABLE 3
Failure loads of anchors with head type B

Series	f_{cc}	F_u [kN] for h in [mm]			F_{u1}[1)] [kN] for h in [mm]		
	MPa	50	150	450	50	150	450
I	32.6	25.8	150.0	1087	25.2	146.3	1060
II	29.7	(40.2)	161.7	1108	(41.1)	165.2	1132
III	33.2	35.6	131.4	1162	34.4	127.0	1123
IV	29.3	27.2	133.3	937.2	28.0	137.1	964.0
		26.1	181.7		26.8	186.9	
V	28.3	21.5	160.7	989.0	22.5	168.2	1035
		30.2	165.7		31.6	173.4	
VI	34.4	29.3	151.5	1221	27.8	143.8	1159
		33.2	167.7		31.5	159.2	
		29.6			28.1		
		35.6			33.8		
Average	31.2	29.4[2)]	160.0	1084	29.0[2)]	156.3[1)]	1079
V [%]	7.9	15.3	10.2	9.8	13.1	12.3	6.8

1) $F_{u1} = F_u \cdot \sqrt{31/f_{cc}}$ 2) without result of Series II

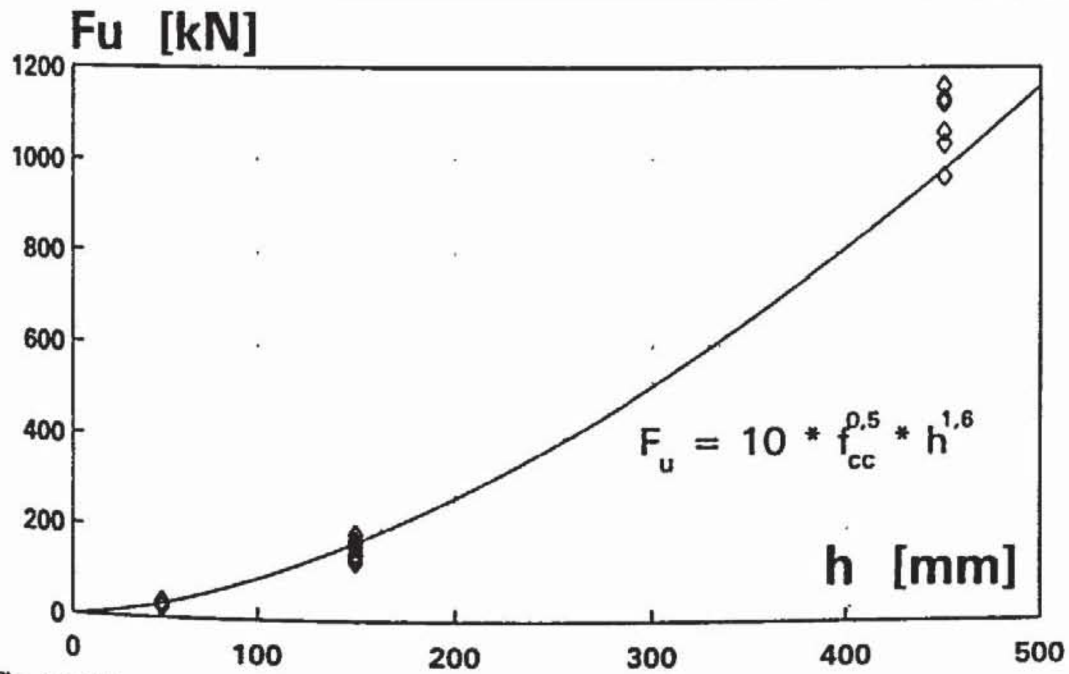

Fig. 3 Failure loads (head type B) as a function of the embedment depth

In Fig. 3 the normalized failure loads are plotted as a function of the embedment depth. The average values can be approximated by Eqn. (1). This equation is sufficiently accurate for practical purposes (compare Table 4).

$$F_u = 10 \cdot f_{cc}^{0.5} \cdot h^{1.6} \qquad (1)$$

DISCUSSION OF RESULTS

In [4] the following empirical equation is proposed. It assumes the greatest possible size effect which will be obtained when applying linear fracture mechanics [5]. The formula is based on approximately 200 results of tests with headed anchors from different sources. The embedment depth was varied between d = 40 mm and d = 525 mm.

$$F_u = 15.5 \cdot f_{cc}^{0.5} \cdot h^{1.5} \qquad (2)$$

In [7] another empirical equation is given, which does not take into account a size effect

$$F_h = 0.96 \cdot f_{cc}^{0.5} \cdot h^2 \, (1 + d_h/h) \qquad (3)$$

According to Bazant's size effect law [8], the nominal concrete strength, $\sigma_N = F_u/A_c$, on the failure cone surface A_c is given by Eqn. (4)

$$\sigma_N = B \cdot f_t \left(1 + h/h_0 \right)^{-0.5} \qquad (4)$$

where B and h_0 are empirical constants. Eqn. (4) predicts a gradual transition from a plastic solution (no size effect) for small embedment depths to a linear fracture mechanics solution (largest size effect) for large embedment depths. Assuming a diameter of the projected cone of 3h [3] the test results yield B = 0.62 and h_0 = 101 mm. In Fig. 4 the ratio $\sigma_N/(B \cdot f_t)$ is plotted as a function of the ratio h/h_0 in double logarithmic scale. It can be seen, that for h = 450 mm the test results are close to the linear fracture mechanics solution. With $f_t = 0.5 \cdot f_{cc}^{0.5}$ and $A_c = \pi \cdot (3h)^2/4$ one gets from Eqn. (4) the following failure load.

$$F_u = 2.2 \cdot f_{cc}^{0.5} \cdot h^2 (1 + h/100)^{-0.5} \qquad (5)$$

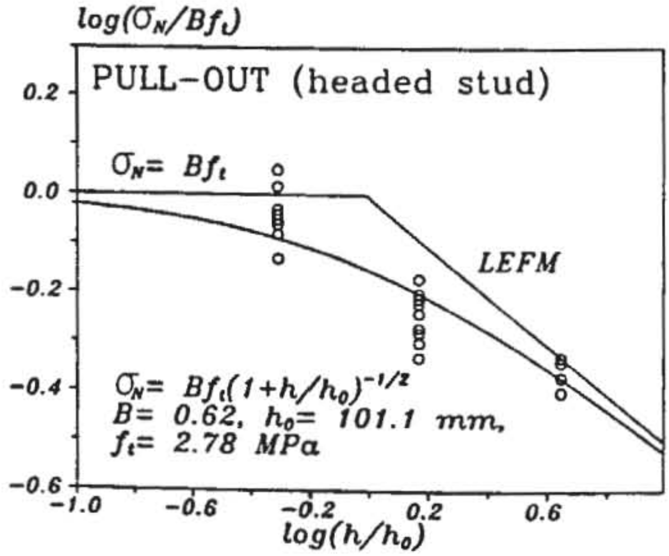

Fig. 4 Size effect of the average tensile stress over the failure cone area

In Fig. 5 the measured failure loads related to the average value for h = 50 mm are plotted as a function of the embedment depth in double-logarithmic scale. In this scale, Eqns. (1) to (3) are straight lines with different slopes and Eqn. (5) gives a slightly curved line. The figure shows, that the size effect law (Eqn. (5)) agrees rather well with the test results. While Eqn. (2) slightly overestimates, Eqn. (3) significantly underestimates the size effect.

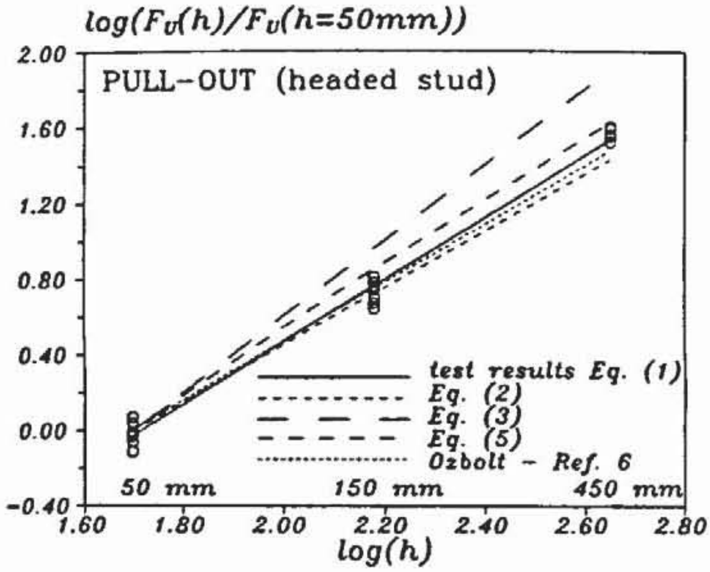

Fig. 5 Related failure loads as a function of the embedment depth

In Table 4 the test results are compared with the predictions according to Eqns. (1) to (3) and (5). As expected, Eqn. (1) gives the best representation of the test results. Eqn. (3) agrees worst with the test results, because the average value of the ratio measured failure load to calculated value decreases significantly with increasing embedment depth and the coefficient of variation of the ratio $F_{u,test}/F_{u,calculated}$ is about 3 times larger than the coefficient of variation of the measured failure loads. Equation (2) is conservative for h = 450 mm.

TABLE 4
Comparison of test results with various predictions

h	average failure load [1]	F_u [kN] predicted according to Eqn. [1]				$F_{u,test}$ / $F_{u,calculated}$ according to Eqn.			
mm	kN	(1)	(2)	(3)	(5)	(1)	(2)	(3)	(5)
50	29.0	29.1	30.5	16.8	25.0	1.00	0.95	1.73	1.16
150	156.3	168.8	158.5	146.6	147.3	0.93	0.99	1.07	0.90
450	1079	979	824	1295	1058	1.10	1.31	0.83	1.20
[1] f_{cc} = 31 MPa					$\bar{x}$	1.0	1.05	1.27	1.03
					V [%]	12.9	17.7	32.9	16.0

In an earlier study [5] headed anchors (h = 130, 260 and 520 mm) were embedded in one large concrete block (d = 600 mm) and loaded in tension. Failure occured by pulling out a concrete cone. In Fig. 6 the failure loads related to the value for h = 130 mm are plotted as a function of the embedment depth in double logarithmic scale. The increase in failure load is almost correctly predicted by Eqn. (1), slightly underestimated by Eqn. (2) and significantly overestimated by Eqn. (3). It should be mentioned that these tests have been criticized because of the too small member depth. However, in the light of the present results, this criticism seems not to be justified.

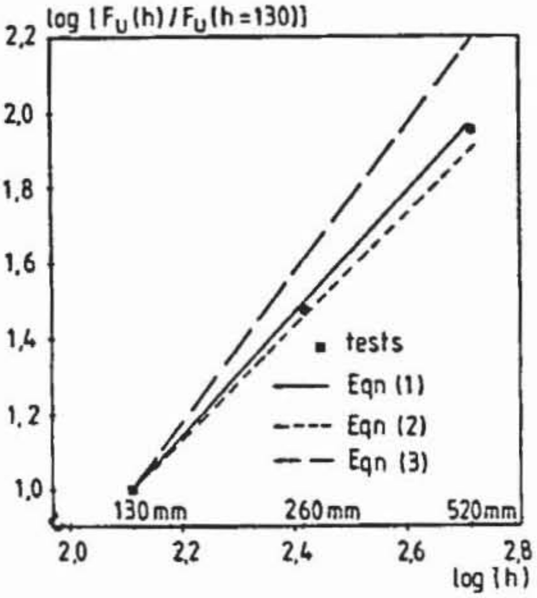

Fig. 6 Related failure loads as a function of the embedment depth, tests according to [5]

In [6], [9] a non-linear finite element simulation of the present tests was performed. While in [6] the investigation was based on the non-local microplane model [10], in [9] a new thermodynamical model was applied. Both material models take non-linear fracture mechanics into account. The results of the two studies compare very favourably. The results of [6] are also plotted in Fig. 5. It can be seen, that they agree quite well with the experimental results.

The size effect might be influenced by the concrete mix. Therefore, similar tests as described here are needed with a variation of the concrete mix.

CONCLUSIONS

Based on the present study, the following conclusions can be drawn

(1) The concrete cone failure load shows a significant size effect which is rather close to the solution according to linear fracture mechanics. This can be explained by the high strain gradient and the relatively small fracture process zone [5, 6].

(2) The size effect should be taken into account in the design of fastenings, because otherwise the strength of fastenings with a small embedment depth is overestimated and those with a large embedment depth is underestimated.

REFERENCES

1. Bouška, P., Červenka, V., Experimental Investigation of Anchoring Bolts, Research report, Klokner Institute, Technical University Prague, 1991.

2. Bouška, P., Experimental Investigation of Anchoring Bolts in 1991, Research report, Klokner Institute, Technical University Prague, 1991.

3. Rehm, G., Eligehausen, R., Mallée, R., Befestigungstechnik, Betonkalender 1988, part 2, pp. 569 - 663, Ernst & Sohn, Berlin, 1988.

4. Eligehausen, R, Ick, U., Mallée, R., Reuter, M., Schimmelpfennig and Schmal: Tragverhalten von Kopfbolzenverankerungen bei Zugbeanspruchung, Bauingenieur, in press.

5. Eligehausen, R., Sawade, G., A fracture mechanics based description of the pull-out behaviour of headed studs embedded in concrete, Fracture Mechanics of Concrete Structures, Report of RILEM TC-90-FMA, Ed. L. Elfgren, Chapman and Hall, London New York, 1989, pp. 281 - 299.

6. Ožbolt, I., Round-Robin Analysis Of Anchor Bolts. Report to RILEM-TC-90-FMA, March 1991.

7. ACI 349-85, Code Requirements for Nuclear Safety Related Concrete Structures, Appendix B, Steel Embedments, American Concrete Institute, Detroit, 1985.

8. Bažant, Z. P., Size effect in Blunt Fracture: Concrete, Rock, Metal. Journal of Engineering Mechanics ASCE, 1984, 110 (4), pp. 518 - 535.

9. Sawade, G. and Eligehausen, R., Analysis of Headed Steel Anchors Embedded in Concrete Using a Non-linear Fracture Model, Proceedings, First International Conference on Fracture Mechanics of Concrete Structures, Breckenridge, June 1992.

10. Bažant, Z. P. and Ožbolt, I., Non-local microplane model for fracture, damage and size effect in structures. Journal of Engineering, Mechanics, ASCE, 1990, 116 (11), pp. 2485 - 2504.

11. RILEM draft recommendation: Determination of the fracture energy of three point bend tests on notched beams. Materials and Constructions, July - August 1985, 106, pp. 285 - 296.